Computers and Concrete, *Vol. 16, No. 1 (2015) 99-123*
DOI: http://dx.doi.org/10.12989/cac.2015.16.1.099

Fragility assessment of RC-MRFs under concurrent vertical-horizontal seismic action effects

Ehsan Noroozinejad Farsangi[1a], Abbas Ali Tasnimi[*2] and Babak Mansouri[3b]

[1]*SERC, International Institute of Earthquake Engineering and Seismology (IIEES), Tehran, Iran*
[2]*Department of Civil and Environmental Engineering, Tarbiat Modares University (TMU), Tehran, Iran*
[3]*ERMRC, International Institute of Earthquake Engineering and Seismology (IIEES), Tehran, Iran*

(Received April 21, 2015, Revised June 29, 2015, Accepted July 7, 2015)

Abstract. In this study, structural vulnerability of reinforced concrete moment resisting frames (RC-MRFs) by considering the Iran–specific characteristics is investigated to manage the earthquake risk in terms of multicomponent seismic excitations. Low and medium rise RC-MRFs, which constitute approximately 80-90% of the total buildings stock in Iran, are focused in this fragility–based assessment. The seismic design of 3-12 story RC-MRFs are carried out according to the Iranian Code of Practice for Seismic Resistant Design of Buildings (Standard No. 2800), and the analytical models are formed accordingly in open source nonlinear platforms. Frame structures are categorized in three subclasses according to the specific characteristics of construction practice and the observed seismic performance after major earthquakes in Iran. Both far and near fields' ground motions have been considered in the fragility estimation. An optimal intensity measure (IM) called Sa, avg and beta probability distribution were used to obtain reliable fragility–based database for earthquake damage and loss estimation of RC buildings stock in urban areas of Iran. Nonlinear incremental dynamic analyses by means of lumped-parameter based structural models have been simulated and performed to extract the fragility curves. Approximate confidence bounds are developed to represent the epistemic uncertainties inherent in the fragility estimations. Consequently, it's shown that including vertical ground motion in the analysis is highly recommended for reliable seismic assessment of RC buildings.

Keywords: RC-MRFs; fragility curve; vertical seismic excitations; NL platforms; beta distribution

1. Introduction

Earthquake hazard identification and structural vulnerability evaluation are the main components of earthquake risk assessment. Earthquake hazard identification is out of the scope of this study, but structural vulnerability evaluation which is a primary concern among the regulatory agencies and engineering professions to determine, classify, and assess the fragility of existing building stock and other structures (dams, bridges, power plants, etc.), is being focused in the

[*] Corresponding author, Professor, E-mail: tasnimi@modares.ac.ir
[a] Ph.D. candidate, E-mail: e.noroozinejad@iiees.ac.ir
[b] Assistant professor, E-mail: mansouri@iiees.ac.ir

http://www.techno-press.org/?journal=cac&subpage=8 ISSN: 1598-8198 (Print), 1598-818X (Online)

current study.

For disaster management purposes, a fragility based assessment that considers local structural properties is required. However, local conditions are usually ignored and vulnerability based assessment studies for structures in different countries are adapted to earthquake hazard estimation and disaster mitigation. (Del Gaudio *et al.* 2015 and Kurmann *et al.* 2013)

Unfortunately, differences in structural characteristics cause significant deviations on damage and loss estimation by influencing the resulting fragility curves. The aim of this study is to provide fragility information to inquire effects of ground motion parameters and Iranian construction practice state on structural vulnerability in the presence of vertical component of earthquake. After the devastating earthquakes that occurred within the last decade, a well-organized and comprehensive Iranian Code of Practice for Seismic Resistant Design of Buildings (Standard No. 2800, 2005) is published. Making use of this comprehensive design code, this study is deemed to be a benchmark for future studies on earthquake damage and loss estimation in urban areas of Iran.

Structural deficiencies of RC buildings stock in Iran can be classified in three groups: Design deficiencies, detailing deficiencies and constructional deficiencies.

Design Deficiencies : In Iran, in rural and even in urban areas, before the 2003 Bam earthquake and releasing the 3rd edition of Iranian Code of Practice for Seismic Resistant Design of Buildings (Standard No. 2800, 2005), it was sometimes difficult to encounter engineered structures. Unfortunately, most of the engineers and architects were not even familiar with earthquake resistant design. The deficiencies due to improper choice of architectural and structural systems in Iran can be listed as follows

- Low lateral resistance and redundancy
- Irregularities in plan and elevation
- Soft story and weak story
- Short Column
- Overhangs
- Strong beam–weak column joints etc.

Detailing deficiencies : The basic principle of detailing is to provide the necessary strength and ductility at critical sections of structural members and at beam-column joints (ACI 318-05). Detailing deficiencies occur mostly due to tendency to violate the code provisions about detailing of members or to disregard the detailing in the design drawings both intentionally and due to ignorance. These deficiencies can be listed as follows

- Insufficient transverse reinforcement
- Insufficient spliced length of bars
- Insufficient beam–column joint reinforcement etc.

Constructional deficiencies : Incorrect site applications due to the lack of supervision and careless contractors result in structures different than initial architectural and engineering design. Some of the constructional deficiencies in Iranian RC build stock are:

- Unqualified workmanship and inferior material quality
- Addition of new members which are not considered in the design stage
- Omission of some structural members that have been considered in the design stage and that are critical for the lateral resistance of the structural system
- Different member sizes that does not comply with the original design drawings
- Insufficient and wrong reinforcement applications etc.

Based on the above mentioned reasons, frame structures in this study are categorized into three subclasses defined below:

Class 1 : The 1st subclass in the current study includes the RC buildings with non-ductile behaviour or the ones with uncertain ductility. Most of the RC-MRFs constructed before 1999 especially in the Middle-East region are categorized in this group. For a better illustration of this subclass, RC buildings with construction, detailing and design deficiencies are included in this class as well. (ACI 318-89)

Class 2 : It represents a large numbers of the buildings stock concerning the RC residential buildings in the world with a specific focus on the Middle-East region. They are generally engineered structures but may violate some fundamental requirements of earthquake resistant design and construction. Based on the past earthquake data, the RC-MRFs in this subclass behave slightly better than the first category, but still need some retrofitting actions for the future seismic events. (ACI 318-99)

Class 3 : The buildings in this subclass are designed according to the latest seismic codes in the last decade and should have adequate structural capacity in terms of strength and ductility in a severe earthquake. Good material quality, earthquake resistant design, and good supervision in the construction stage result in reliable performance levels. In this study the performance of this subclass is going to be monitored in terms of vertical earthquake excitation as well, to make sure they will behave properly for the future earthquakes. (ACI 318-05)

To consider these subclass properties in the analytical models beside the design differences, a classification based on the material properties is also carried out. Variability in structural strength and stiffness has been of major interest by a number of probabilistic studies of RC members and systems (Dymiotis *et al.* 1999, Lee and Mosalam 2004). As suggested by these studies, the random variables that represent the variability in material characteristics are considered as concrete strength (f'_c) and steel yield strength (f_y).

As mentioned, the main concern of this study is to define the fragility levels of the current RC-MRFs in Iran. Fragility functions are in general derived using a variety of approaches such as field observations of damage, static structural analyses, or judgment (e.g., Kennedy and Ravindra 1984, Kim and Shinozuka 2004, Calvi *et al.* 2006, Villaverde 2007, Porter *et al.* 2007, Shafei *et al.* 2011 and Casotto *et al.* 2014), but here the focus is on so-called analytical fragility functions developed from nonlinear dynamic structural analysis (Kurmann *et al.* 2013, Casotto *et al.* 2014 and Jeon *et al.* 2015). Unlike some other methods, in the case of analytical fragility functions the analyst has control over the data collected, by means of choosing the intensity measure (*IM)* levels at which analysis is performed and the number of analyses performed at each level. The fragility curves generated at the final phase of this study provide a reliable database for earthquake damage and loss estimation of RC buildings such as those stock in Iran.

2. Current seismic design philosophy

Many codes suggest scaling a single spectral shape, originally derived for horizontal components to deal with vertical earthquake motion. This implies that both components of motion have the same frequency content, which is clearly not the case.

A procedure was originally proposed by Newmark *et al.* (1973) and has since been widely used in the seismic codes. It was suggested that the average peak vertical-to-horizontal spectral ratio could be taken as 2/3. This implies that the vertical-to-horizontal ratio is also 2/3 assuming constant amplification. Recent studies by Abrahamson and Litehiser (1989) and Ambraseys and Simpson (1995) confirm that the 2/3 rule is unreasonable. Evidence from the Loma Prieta

earthquake of 1989, the Northridge earthquake of 1994, the Morgan Hill earthquake of 1984, the Nahanni earthquake 1985 and the Kobe earthquake of 1995 confirm this, all with of vertical to horizontal peak ground acceleration (V/H) ratios well in exceedance of 1.0. It is clear that this ratio is magnitude, distance and frequency dependent and should be a variable in code design.

3. Vertical component of ground motions

Vertical component of the strong ground motion is mainly associated with body waves: vertically propagating compressional waves (i.e., P-waves) and horizontally propagating dilatational waves (i.e., S-waves). Compared to the horizontal component, vertical motion may be richer in high-frequency content in the near field of an earthquake fault. As the distance from the source increases, difference in the frequency content between horizontal and vertical components becomes much smaller as a result of faster attenuation of high frequencies with distance, and mixing of horizontal and vertical motions due to nonhomogeneities along the wave path.

A common perception in engineering practice is that intensity of vertical ground motion is lower than that of the horizontal; thereby the V/H ratio, is assumed to remain less than unity. (Bozorginia and Campbell 2004)

In Fig. 1 the authors presented the plot of the V/H ratio against the magnitude of the events for the large PEER-NGA database of earthquake records in the range of 5-7.9 M_w. It may be seen that the median V/H ratios is about 1.1 for the records with Mw≥5.0 and EpiDist.≤100 km which is much higher than the commonly accepted value of 0.67. The maximum V/H ratio in the subset is close to 7.0. This data point corresponds to the 1979 Imperial Valley earthquake (M_w = 6.5) and to the El Centro 6th station, which recorded peak vertical ground acceleration of more than 1.6*g*. Besides that, the maximum vertical acceleration exceeding 2.0 *g* was recorded during the Nahanni earthquake of 1985. This motion produced the vertical-to-horizontal peak ground acceleration ratio (V/H) of at least 2.0.

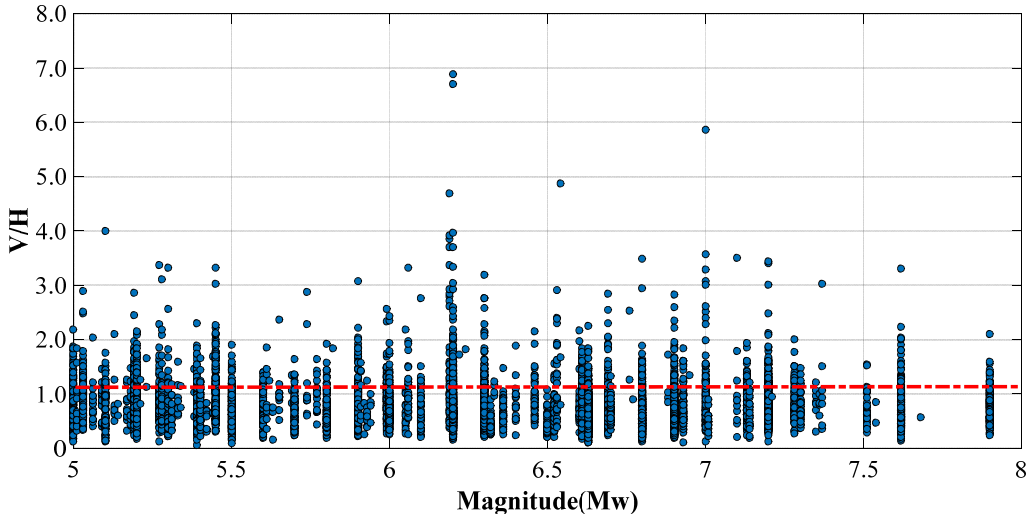

Fig. 1 Ratios of peak vertical to horizontal acceleration (V/H) plotted against moment magnitude

Table 1 Earthquake Records used in this study

Earthquake record	Date	Magnitude(Mw)
Chi-Chi	1999	7.6
Kocaeli	1999	7.4
Duzce	1999	7.1
Loma Prieta	1989	7.0
Kobe	1995	6.9
Northridge	1994	6.7
Erzincan	1992	6.7
Bam	2003	6.6
Zarand	2005	6.4
Morgan Hill	1984	6.2

The exercises conducted on different ground motion databases collectively confirm that V/H ratio may show significant variations, which depend on source and site characteristics and on seismic radiation pattern. Though not all earthquakes and their corresponding data from the near-fault region substantiate that V/H ratio is larger than unity, many data points confirm the opposite; hence influences of vertical component should not be ignored when seismic demands on structural components are assessed. (Grazier 2006, Fujita and Takewaki 2009)

Damage consistent with a high level of vertical acceleration was observed in the 1994 Northridge earthquake. The report from EERI (1995) highlighted cases of brittle fracture induced by direct compression, or by reduction in shear strength and ductility due to variation in axial forces arising from the vertical motion. For first mode vertical response, the reduction in axial force in columns or walls was more significant for higher storeys, since it represents a larger relative change in the pre-existing static axial load. Interior columns were shown to be more vulnerable, and vertical oscillations of slabs at their natural period caused considerable damage. (Broderick and Elnashai 1995).

4. Selection of strong ground motions

Fifty set of ground motions from ten devastating earthquakes having a PGA greater than 0.3 and V/H ratio larger than 0.6 with moment magnitude (M_w) greater than 6.0 were compiled into a database (Table 1). All records were taken from stations within 20 km of the fault rupture for the near-fault analysis and records outside 20 km for far-fault analysis. Most of ground motions used in the fragility assessment here are the ground motions selected for the ATC-63 project (ATC 2007). The ground motion acceleration records were obtained from the PEER Next Generation Attenuation (NGA) database.

5. Fragility estimate

Fragility is the conditional probability of a building reaching or exceeding a certain performance level for a given ground motion parameter. Following the conventional notation in structural reliability theory (Ditlevsen and Madsen 1996, Kurmann *et al.* 2013, Lee *et al.* 2014, Del Gaudio *et al.* 2015), the limit state function for the building is written as Eq. (1).

$$g\left(C, IM; \mu\right) = C - D(IM; \mu) \tag{1}$$

Where *IM* is the seismic intensity parameter, μ represents the vector of unknown parameters of the demand model, and *C* and *D* represent the capacity and demand of the building, respectively. Using Eq. (2), the fragility for the building is written as Eq. (2).

$$F\left(IM; \mu\right) = P[\{g(C, IM; \mu) \le 0\} \big| IM] \tag{2}$$

The uncertainty in the event $g(C, IM; \mu) \le 0$ for given *IM* arises from the inherent randomness in the capacity *C*, the inexact nature of the limit state function, and the uncertainty inherent in the parameters μ of the demand models. (Ramamoorthy *et al.* 2006a, Borgonovo *et al.* 2013)

In order to model for the epistemic uncertainty associated with fragility at a given shaking intensity, a beta probability distribution is used. The choice of beta distribution is natural due to the fact that the variation in probability can be bounded between the two values (i.e., 0% and 100%), and it can be skewed towards either end depending upon the parameters of the distribution; it has also already been identified as a suitable distribution to model the uncertainty associated with the damage factor at a given intensity (ATC 1985, Sudret *et al.* 2014, Baker 2015).

6. Typologies of buildings considered and description of the structural models

This study refers to two national codes for the design of RC buildings. These are the various versions of the Iranian national Building Code for Design and Construction of RC Structures(Part 9) and Iranian Code of Practice for Seismic Resistant Design of Buildings (Standard No. 2800) that state the minimum requirements for structures and structural components to be built in seismic prone areas.

Since number of stories is deemed to be important regarding the seismic response of RC frame structures, it is considered as a major parameter in this study. Hence 3, 5, 7, 9 and 12 story Moment resisting frame models are constructed. The analytical models considered cover the low–and mid–rise RC frame structures population, which represents the majority of residential buildings in Iran. Story height of 3.0 meters and bay width of 5, 6 and 7 meters are assumed in accordance with the common practice.

A reference code is assigned to each frame to be addressed in the next sections. Reference codes of the RC-MRFs in this study are given in the form of "*m*S*n*B-E/NE*r*", in which "*m*S" represents the "*m*" number of stories "S", "*n*B" indicates "*n*" number of bays "B". "E" and "NE" indicate the equal and non-equal bay structures respectively. When NE follows by a digit that represents by "*r*" indicates that the configuration of the models are the same, but the sequence of non-equal bay may differ. Table 2 Provides relevant information for each structure considered in this paper.

Design details are presented for 3S3B-E frame in Fig. 2 and the structural details for other structures are summarized in Table 3. The archetypes are limited to RC moment frames without infill walls, and are regular in elevation and plan, without major strength or stiffness irregularities. The designs also satisfy all relevant building code requirements, including maximum and minimum reinforcement ratios and maximum stirrup spacing. (ACI 318-89, 318-99 and 318-05).

Table 2 Bays configuration for the studied RC-MRFs

No.	Equal Bays Frames		No.	Non-Equal Bays Frames	
	Frame Name	c/c of Bays		Frame Name	c/c of Bays
1	3S3B-E	@5 m	*14*	3S3B-NE	@5-7-5
2	5S3B-E	@5 m	*15*	12S3B-NE	@5-7-5
3	7S3B-E	@5 m	*16*	3S4B-NE	@7-5-5-7
4	9S3B-E	@5 m	*17*	12S4B-NE	@5-7-7-5
5	12S3B-E	@5 m	*18*	5S5B-NE1	@5-5-7-5-5
6	3S4B-E	@6 m	*19*	5S5B-NE2	@7-5-7-5-7
7	5S4B-E	@6 m	*20*	7S5B-NE	@7-5-7-5-7
8	7S4B-E	@6 m	*21*	9S5B-NE1	@7-5-5-5-7
9	9S4B-E	@6 m	*22*	9S5B-NE2	@7-5-7-5-7
10	12S4B-E	@6 m	*23*	12S5B-NE	@7-5-7-5-7
11	7S5B-E	@6 m			
12	9S5B-E	@6 m			
13	12S5B-E	@6 m			

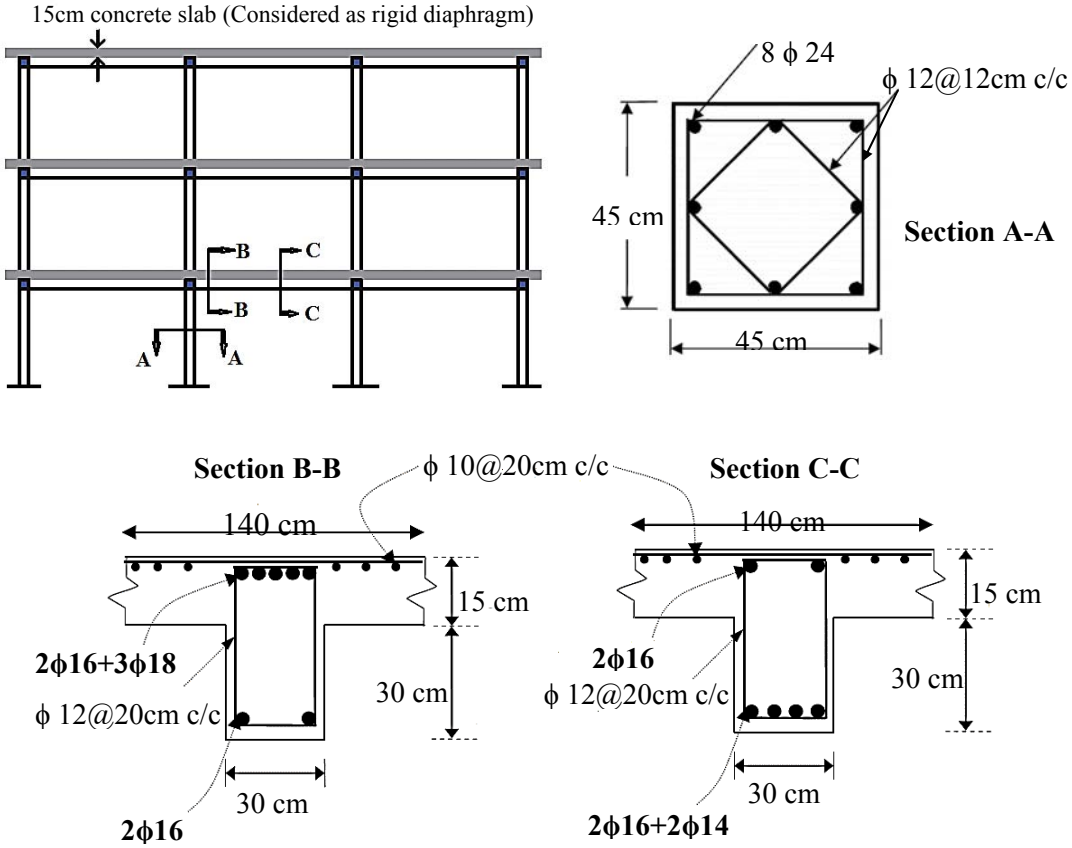

Fig. 2 Cross-sections and reinforcement details for beams and columns for 3S3B-E frame (class 3)

Table 3 Design characteristics of the studied RC Frames

No. of Storey	Classifications	Column size[1] (m×m)	Column reinforcement ratio, ρ	Column tie spacing [2,3] (cm)	Beam size[4] (m×m)	Beam reinforcement ratios ρ (ρ')	Beam tie spacing (cm)
3	Class 1	0.40×0.40	0.024	30	0.30 ×0.40	0.006(0.011)	35
	Class 2	0.45×0.45	0.020	15	0.30 ×0.45	0.006(0.010)	25
	Class 3	0.45×0.45	0.018	15	0.30 ×0.45	0.006(0.010)	20
5	Class 1	0.45×0.45	0.021	30	0.30 ×0.40	0.007(0.014)	35
	Class 2	0.50×0.50	0.019	15	0.30 ×0.45	0.007(0.012)	20
	Class 3	0.50×0.50	0.017	15	0.35 ×0.50	0.005(0.008)	15
7	Class 1	0.50×0.50	0.023	25	0.40 ×0.45	0.006(0.013)	30
	Class 2	0.55×0.55	0.021	15	0.40 ×0.50	0.006(0.011)	15
	Class 3	0.60×0.60	0.018	10	0.45 ×0.50	0.006(0.011)	15
9	Class 1	0.60×0.60	0.018	25	0.45 ×0.50	0.007(0.013)	30
	Class 2	0.65×0.65	0.017	15	0.45 ×0.55	0.006(0.010)	15
	Class 3	0.70×0.70	0.016	10	0.45 ×0.55	0.004(0.009)	12
12	Class 1	0.70×0.70	0.025	20	0.45 ×0.55	0.006(0.011)	25
	Class 2	0.75×0.75	0.021	15	0.45 ×0.60	0.006(0.009)	15
	Class 3	0.75×0.75	0.017	10	0.50 ×0.60	0.005(0.009)	12

[1] Column properties vary over the height of the structure and are reported here for an interior first and second-stories columns.
[2] Configuration of transverse reinforcement in each member depends on the required shear strength. There are at least two ϕ10 bars at every location.
[3] Configuration of transverse reinforcement in Class3 RC frames depends on the required shear strength. All ties have seismic detailing and use ϕ12 bars (ACI 318-05).
[4] Beam properties vary over the height of the structure and are reported here are for the first and second-stories beams.

6.1 Hysteretic model used

The hysteretic model for beam/column used in this study was developed by Ibarra *et al.* (2005). Fig. 3 shows the trilinear monotonic backbone curve and associated hysteretic rules of the model, which provide for versatile modeling of cyclic behavior. An important aspect of this model is the negative stiffness branch of post-peak response, which enables modeling of strain-softening

behavior associated with concrete crushing, rebar buckling and fracture, and bond failure. The model also captures four basic modes of cyclic deterioration: strength deterioration of the inelastic strain-hardening branch, strength deterioration of the post-peak strain-softening branch, accelerated reloading stiffness deterioration, and unloading stiffness deterioration. Additional reloading stiffness deterioration is automatically incorporated through the peak-oriented cyclic response rules. Cyclic deterioration is based on an energy index that has two parameters: normalized energy-dissipation capacity and an exponent term to describe how the rate of cyclic deterioration changes with accumulation of damage. Pinching model is utilized for class 1 which has uncertain ductility and peak-oriented model is used for class 2 and 3 as the ductile behaviour is considered in their design stage.

7. Results and discussion

The dynamic response time history analyses were performed with selected records described in section 4. The extracted results are discussed accordingly.

7.1 IM Selection for the incremental dynamic analysis (IDA)

The damage potential of earthquake ground motion is usually characterized by a ground motion parameter called the intensity measure (IM) in seismic vulnerability assessment. A good IM should meet the requirement of efficiency and sufficiency. Efficiency means the ability to accurately predict the response of a structure subjected to earthquakes (i.e., small dispersion of structural response subjected to earthquake ground motions for a given IM). And a sufficient IM is defined as one that renders structural responses subjected to earthquake ground motions for a given IM conditionally independent of other ground motion properties (i.e., no other ground motion information is needed to characterize the structural response). An efficient IM results in smaller variability of structural response, which implies fewer ground motion input for performance evaluation. Sufficiency of an IM is desirable because it reduces the complexity of record selection procedure based on seismic environment (i.e., magnitude, distance, site conditions, etc.) (Lucco and Cornell 2007).

In the past, peak ground acceleration (PGA) was commonly used as an IM. Simplicity is the main advantage of PGA, but it results in great dispersion of structural response. More recently, the spectral acceleration at the first mode period of the structure, $S_a(T_1)$, has been thoroughly studied and became very popular. This IM contains ground motion spectral information as well as dynamic characteristics of structure, so it's more efficient and sufficient than PGA (Hwang and Huo 1997, Shinozuka *et al.* 2000). However, earthquake disaster experience and strong ground motion data show that the structural seismic response depends on ground motion amplitude, spectrum, and duration characteristics simultaneously, and the different combinations of these three elements determine the degree of safety of the structure. Numerous studies also showed that scalar-valued IM such as $S_a(T_1)$ couldn't comprehensively describe the complex nature of earthquake ground motions, resulting in great uncertainty in vulnerability assessment (Shome *et al.* 1998, Song and Ellingwood 1999, Ellingwood 2001, Kafali and Grigoriu 2004, Schotanus *et al.* 2004). In this study, in order to accurately characterize the ground motion potential, a new proposed IM by (Bianchini *et al.* 2009) which is the geometric mean of pseudo-spectral acceleration ordinates over a certain range of periods, $S_{a,avg(}T_1,\ldots,T_n)$, or briefly $S_{a,avg}$, is used as an optimal scalar IM to

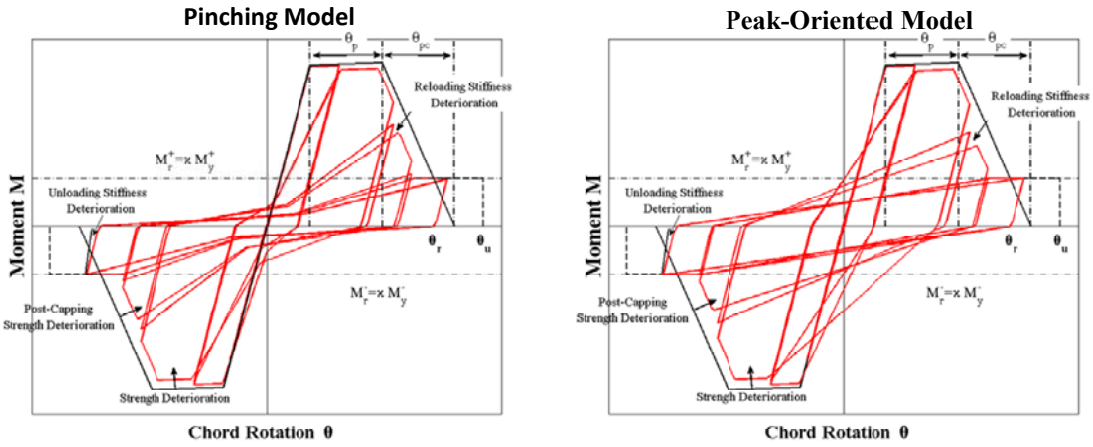

Fig. 3 Monotonic and cyclic behavior of component model used in study (Ibarra *et al.* 2005)

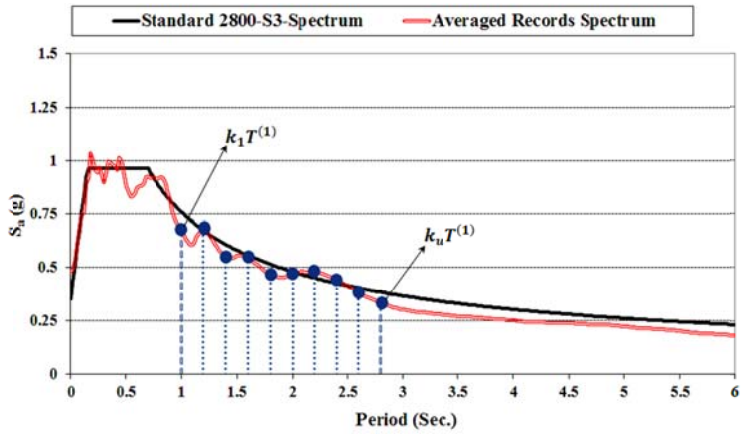

Fig. 4 Schematic definition of $S_{a,avg}$ based on the selected strong motion records

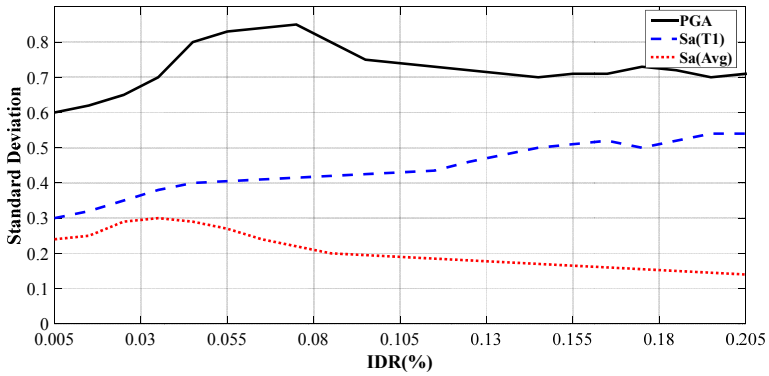

Fig. 5 Comparison of standard deviation in the IDA curves for different IM

predict inelastic structural response of buildings subjected to recorded ground motions. The formulation for this IM is given in Eq. (3).

$$S_{a,avg}\left(T_1,\ldots,T_n\right)=\sqrt[n]{\left(\prod_{i=1}^{n}S_a(T_i)\right)} \tag{3}$$

It's proven that, for multi-degree-of-freedom systems, $S_{a,avg}$ can be calculated using ten points logarithmic spaced in the interval $T_1,...,T_n$. Furthermore, they supposed that T_1 and T_n are unknown, but tied to the fundamental period of the structure, $T^{(1)}$. So, the average of spectral accelerations is calculated such that $T_1 = k_1T^{(1)}$ and $T_n = k_uT^{(1)}$, where k_1 and k_u are constants specifying lower and upper bounds, respectively, relative to $T^{(1)}$. With these assumptions, Eq. (4) can be written as

$$S_{a,avg}=\sqrt[10]{\left[S_a\left(k_1T^{(1)}\right)\times\ldots\times S_a\left(k_uT^{(1)}\right)\right]} \tag{4}$$

The constant k_1 is chosen to vary between $T_{low}/T^{(1)}$ and 1, whereas k_u between 1 and $T_{upp}/T^{(1)}$, where T_{low} and T_{upp} are, respectively, the lower and the upper periods of the elastic spectrum (Fig. 4).

To check the effectiveness of the used IM, a comparison has been made amongst the $S_{a,avg}$, $S_a(T_1)$ and PGA to make sure the selected IM is appropriate both in terms of efficiency and sufficiency. The comparison in terms of maximum interstorey drift ratio (IDR) vs. Standard deviations of the IDA results is illustrated in Fig. 5. Results make it clear that, $S_{a,avg}$ is much more superior and reliable compared to conventional IM.

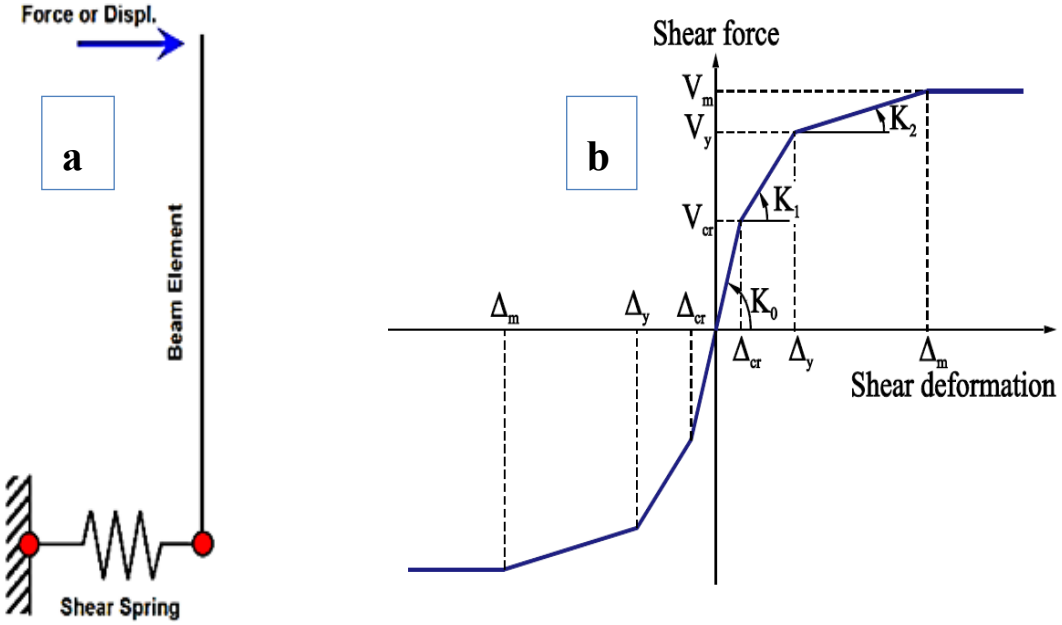

Fig. 6 Shear spring model used in the NL platforms

7.2 Structural modeling and response measures

The Mid-America Earthquake Center program (ZEUS-NL) and The Pacific Earthquake Engineering Research Center program (OpenSees) were utilized to perform the analyses for the selected structures. ZEUS-NL platform is an advancement of the earlier analysis packages ADAPTIC and INDYAS developed by MAE, which is an inelastic fiber-based analysis package which was specifically developed for earthquake engineering applications (Elnashai *et al.* 2004). OpenSees is an open-source platform which was developed in the Berkeley University for the seismic response simulations (Mazzoni *et al.* 2007).

Structural failure may occur due to the attainment of member or system level limit states. Thus, in this study the structural response was investigated at both the global and the local levels. Interstorey drift was considered as a global failure criterion, while the steel and concrete stress/strains of structural members were monitored to assess failure on a local level. The effect of vertical ground motion on axial force was also investigated.

To account for shear deformation, the elements were modeled with a shear spring (Lee and Elnashai 2001) in parallel with an inelastic beam element as shown in Fig. 6(a). The primary curve of the shear spring is defined by a multilinear symmetric relationship that accounts for the cracking, yielding, and ultimate states, as shown in Fig. 6(b). Response 2000 (Bentz 2000) was employed to define the primary curve. Response 2000 is fiber analysis program for RC members employing the Modified Compression Field Theory developed at the University of Toronto (Vecchio and Collins 1986).

7.3 Limit states definition

Interstorey drift ratio (IDR) is considered to be the primary and most important global collapse criterion. This failure criterion places an upper limit on the acceptable storey drift of the structure. The IDR is defined as the ratio of relative displacement (Δ_i-Δ_{i-1}) between successive storeys to the storey height (h_i) (Eq. (5)).

$$(\mathrm{IDR})_i = \frac{\Delta_i - \Delta_{i-1}}{h_i} \tag{5}$$

In the recent years, several values for the IDR collapse limit have been suggested by seismic codes and guidelines (SEAOC-Vision 2000 1995, NEHRP–FEMA 273 1996), but it is unrealistic to assess the response of various structures using a single collapse criterion. Therefore, to better assess the performance of various structures with different configurations and ductility levels, three limit states termed ‘Serviceability’, ‘Life Safety’, and ‘Partial Collapse’ are used in this study. The first cracking in concrete which usually refers to immediate occupancy is ignored due to the lower importance compared to other 3 limit states. The limit states are defined as follows:

- *Slight Damage:* First cracking in concrete
- *Minor Damage (Serviceability)*: first yielding of steel
- *Moderate Damage (Life Safety)*: concrete strain corresponding to maximum confined concrete stress, ε_{cc} given by Eq. 6 and illustrated in Fig. 7.

$$\varepsilon_{cc} = \varepsilon_{co}\left[1 + 5\left(\frac{f'_{cc}}{f'_{co}} - 1\right)\right] \tag{6}$$

Table 4 Determination of IDR% limit of 1st storey for all the structural models in various subclasses

Model Name	IDR (%)								
	Minor Damage			*Moderate Damage*			*Extensive Damage (Partial Collapse)*		
	Class 1	*Class 2*	*Class 3*	*Class 1*	*Class 2*	*Class 3*	*Class 1*	*Class 2*	*Class 3*
3S3B-E	0.15	0.23	0.28	0.38	1.13	1.70	1.08	2.23	3.35
3S3B-NE	0.17	0.27	0.33	0.41	1.26	1.95	1.03	2.12	3.29
3S4B-E	0.21	0.34	0.44	0.54	1.72	2.75	1.17	2.40	3.84
3S4B-NE	0.24	0.39	0.51	0.43	1.43	2.36	1.25	2.56	4.22
5S3B-E	0.24	0.41	0.56	0.60	2.05	3.49	1.50	3.05	5.19
5S4B-E	0.22	0.38	0.54	0.61	2.12	3.71	1.55	3.13	5.48
5S5B-NE1	0.22	0.39	0.59	0.64	2.31	4.16	1.61	3.23	5.81
5S5B-NE1	0.24	0.45	0.71	0.54	1.98	3.66	1.71	3.41	5.21
7S3B-E	0.31	0.59	0.97	0.43	1.16	2.20	1.19	2.36	4.48
7S4B-E	0.27	0.53	0.91	0.31	1.20	2.34	1.36	2.70	5.27
7S5B-E	0.30	0.55	0.81	0.57	2.05	2.97	1.39	3.02	4.56
7S5B-NE	0.46	0.81	1.25	0.51	1.72	2.41	1.24	2.68	3.91
9S3B-E	0.31	0.54	0.82	0.45	1.56	2.11	1.47	3.15	4.44
9S4B-E	0.37	0.62	0.92	0.50	1.67	2.17	1.69	3.58	4.87
9S5B-E	0.44	0.72	1.04	0.59	1.93	2.41	1.54	3.23	4.23
9S5B-NE1	0.53	0.83	1.18	0.65	2.05	2.46	1.66	3.46	4.36
9S5B-NE2	0.33	0.51	0.75	0.50	1.53	1.76	1.44	2.97	3.59
12S3B-E	0.32	0.48	0.73	0.53	2.14	2.35	2.02	4.12	4.78
12S3B-NE	0.41	0.59	0.93	0.65	2.18	2.29	1.92	3.87	4.30
12S4B-E	0.41	0.56	0.91	0.70	2.21	2.21	2.03	4.05	4.29
12S4B-NE	0.44	0.58	0.97	0.67	1.78	1.69	1.59	3.15	3.18
12S5B-E	0.55	0.71	1.22	0.78	1.53	1.46	1.87	3.67	3.52
12S5B-NE	0.63	0.78	1.38	0.73	1.67	1.78	1.79	3.48	3.17
Average	0.34	0.53	0.81	0.55	1.74	2.45	1.53	3.10	4.32

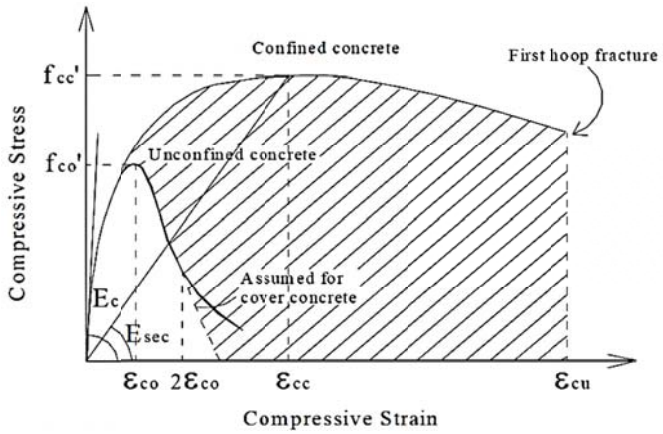

Fig. 7 Stress-strain model proposed by (Mander *et al.* 1988) for confined and unconfined concrete

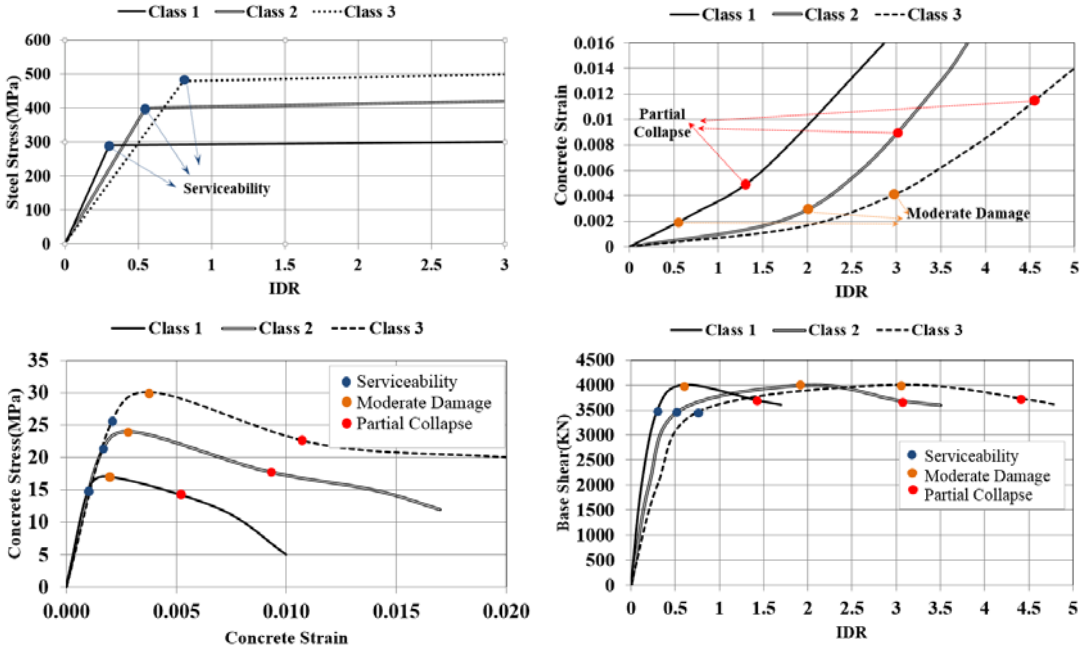

Fig. 8 Determination of IDR limit of 1st storey for 7S5B-E

- *Extensive Damage (Partial Collapse):* maximum confined concrete strain given by (Fig. 7)

$$\varepsilon_{cu} = 0.0035 + 0.1\alpha\omega_w \tag{7}$$

Where ω_w is the mechanical volumetric ratio of confining hoop = $\rho_w f_{yw}/f_c$ and $\alpha=\alpha_n\times\alpha_s$ is the confinement effectiveness coefficient, where

$$\alpha_n = 1 - \frac{\sum w_i^2 / 6}{A_{cc}} \tag{8}$$

$$\alpha_s = \left(1 - \frac{s}{2d_c}\right)^2 \tag{9}$$

For more rigorous analysis, IDR limit per each individual structure from push-over analysis with loading profile of first mode shape was estimated. As shown in Fig. 8, the 1st storey drifts corresponding to each limit state for one of the 7 storey-regular frame buildings (7S5B-E) are (0.30%, 0.57% and 1.39%), (0.55%, 2.02% and 3.05%) and (0.81%, 2.97% and 4.56%) for Class1, 2 and 3 respectively. It is assumed that these limit states can be also applicable to the remaining stories. The results for other RC-MRFs are summarized in Table 4.

7.4 The effect of vertical component on axial loads of columns

For one of the seven storey models (7S5B-E), the variation of the averaged maximum values of the axial loads of the columns on each floor under three earthquake records with different V/H

ratio are shown in Fig. 9. As can be seen, the variation of axial loads at each story level of the interior columns under the effect of horizontal ground motion, had little change compare to that under gravity loads. But there are more changes in the case of interior columns (Fig. 10).

It is clear that the effect of combined horizontal and vertical ground motion, increases the peak value of exterior columns evidently, while the variation of the peak value of interior columns was particularly significant. This significant fluctuation of axial force increased the possibility of the shear failure in the columns.

The tension force along the columns' length did not occur in all the exterior and interior columns under horizontal ground motion. But the action of vertical ground motion made the tension force occur in the columns and the maximum tension force mostly occurred in the middle and upper columns of the structure.

7.5 Plastic hinges formation and distribution

In this section development of plastic hinges in beams and columns corresponding to various V/H is studied. V/H are taken as 0.75 and 1.25 and the comparison is made when the frames are under the horizontal excitation only. The distribution of the hinges are plotted at three states. The first state is corresponding to the initial beam hinges formation, the second state is related to the first column hinge formation at the structures base and the third is considered as the plastic hinges formation in all base columns

As shown in the Fig. 11, under horizontal ground motion, the first hinges formed at the beam-end of the 1st, 2nd and 3rd floors successively and then progressed toward upper floors. Then the column hinge developed at the lower end of the fourth (left to right) column on the 1st floor and then progressed toward upper floors and some hinges developed at columns on the 2nd, 5th and 6th floors respectively. Finally, all the columns lower ends in the 1st floor hinged.

In terms of multicomponent seismic excitation including the vertical component, the hinge formation and sequence are very much different to the previous case. When inputting combined horizontal and vertical ground motion, the beam hinges developed in the middle and upper floors first and then propagates towards all the other stories. Another important finding is that, the ratio of V/H excitation has direct effect on the hinge formations. The column hinges notably increased especially at the middle floors for higher V/H values (Figs. 12 and 13). And the column hinges concentrated at the interior columns while the hinges at the exterior columns were less.

So, when inputting combined horizontal and vertical ground motions, the frame structure are more likely to form a mechanism of beam-column hinge of which the column hinge is principal. Thus the interior columns especially in the middle floor would be the weak part, which might change the collapse mechanism of the structure. The summarized results are given in Table 5.

7.6 Simulate collapse modes in class 1

To investigate side-sway collapse for the benchmark buildings, incremental dynamic analyse (IDA) (Vamvatsikos and Cornell 2002) were performed. With the goal to evaluate the collapse performance, the IDA was performed with the large set of records in the suite assembled for the 2% in 50 years motion, which was the highest intensity level for which a ground motion suite was assembled in this study. For the IDA simulations, side-sway collapse is defined as the point of dynamic instability when story drift increases without bounds for a small increase in the ground motion intensity. Based on the assumptions of existing methodologies, collapse was defined by

two different methods: (1) the IDA curve may become a flat line, which means that the solution has not converged completely, or (2) the rate of decrease in stiffness with increasing record intensity exceeds a prescribed IDR, and is considered doubtful beyond 10% (Cornell *et al.* 2005).

Fig. 14 shows the various collapse mechanisms predicted by nonlinear dynamic analysis for the RC-MRFs represent non-code-conforming buildings and class 1 and the strong-column weak-beam (SCWB) code provision (ACI 318-05) was not imposed in the design. As shown in the Fig. 14, there are four distinct failure modes for low and mid-rise buildings with different intensities, which depend on the ground motion record.

7.7 Collapse modes in class 2 and 3

We found that the strong-column weak-beam (SCWB) ratio increases the collapse capacity to the extent that it improves the collapse mechanism and causes the damage to be spread over more stories of the building. The aim of the SCWB design provision is to avoid localized story mechanisms and thus attain more distributed failure mechanisms. As specified in (ACI 318-05 and 318-11) and comparable codes, this provision does not fully prevent column hinging and incomplete mechanisms, but only helps to delay column hinging and to spread the damage over more stories of the building. The SCWB ratio is assumed to be 1.2 in most of the Seismic codes.

Fig. 15 illustrates this point by showing the predominant collapse mechanisms for each design SCWB value for the 5-story buildings representative of mid-rise RC-MRFs. This shows that the collapse mechanism improves for increasing SCWB value, and a complete mechanism develops for SCWB≥2.0; any further increase above 2.0 no longer benefits the collapse mechanism. This point where the collapse mechanism becomes complete is close to the point where increases in the SCWB ratio stops improving the collapse capacity (Fig. 15).

7.8 Effects of bay spacing

The bay spacing makes little difference in the collapse performance under the horizontal excitation but for the coupled horizontal-vertical case as the shear demand is increasing, shear failure is more likely to happen in structural members before the structure reaches the global collapse state. Shear failure is initiated by inclined cracks that are influenced not only by shear force, but also moments and axial loads.

If we compare the collapse results for buildings with 5 m and 7 m bay spacing under horizontal earthquake component, there seems to be a trend, but when we looked at the details of each building design, we found that the differences in performance are more the results of random differences in design decisions rather than of the bay spacing. The one slight influence of bay spacing occurs when an increase in bay spacing triggers the joint shear requirement to control the design. When this occurs, the column sizes are often increased to accommodate joint shear demands; which in turn reduces axial stress and increases the rotation capacity of the columns. In the end, this only improved the collapse performance a slight amount.

7.9 Probabilistic structural capacity

To estimate the seismic fragility, the capacity values must be specified in a probabilistic sense. The deterministic seismic structural capacity value corresponding to the damage levels from IDA are considered as the median capacity value. Uncertainty in estimation of the structural capacity

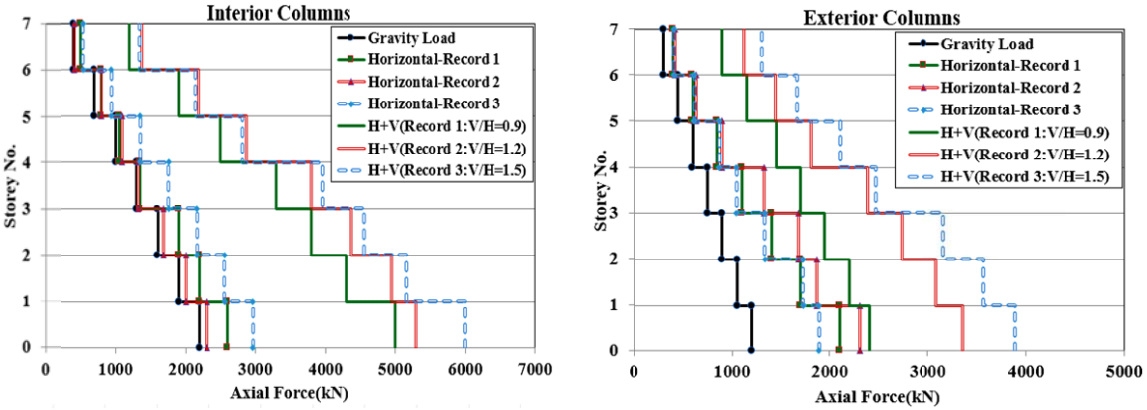

Fig. 9 The peak value of the axial loads of the columns on each floor, Frame (7S7B-E)

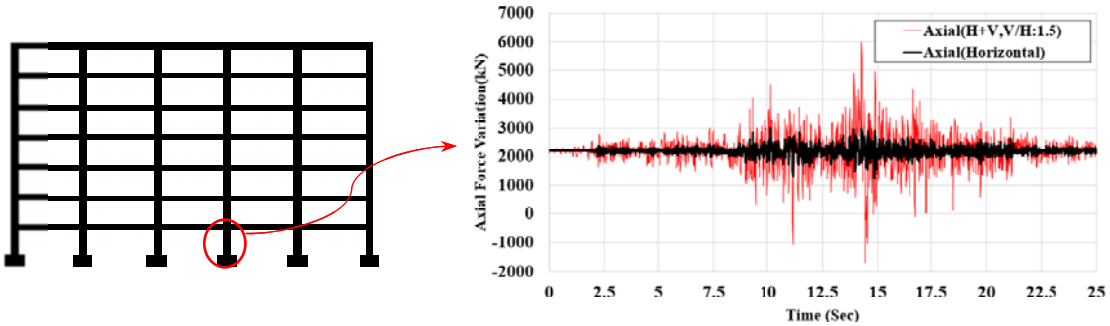

Fig. 10 Variation in axial load of interior column in terms of vertical excitation, Frame (7S5B-E)

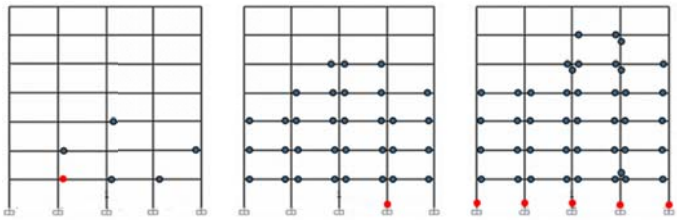

Fig. 11 Plastic hinges formation for horizontal excitation at various states of behaviour

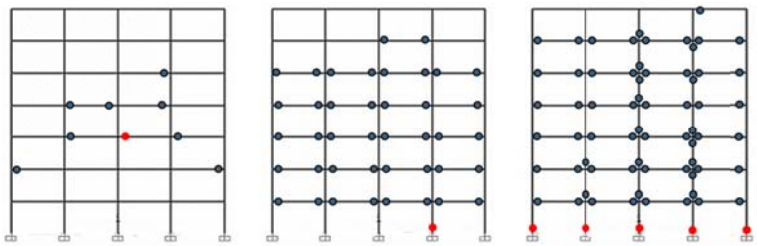

Fig. 12 Plastic hinges formation for H+V(V/H=0.75) excitation at various states of behaviour

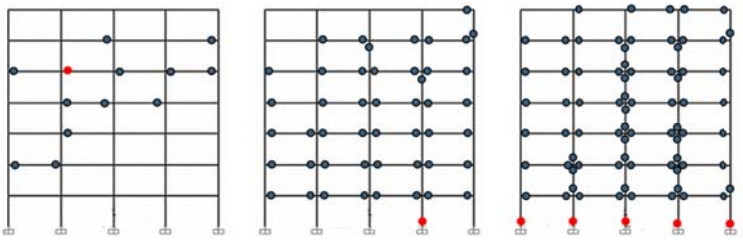

Fig. 13 Plastic Hinges formation for H+V(V/H=1.25) excitation at various states of behaviour

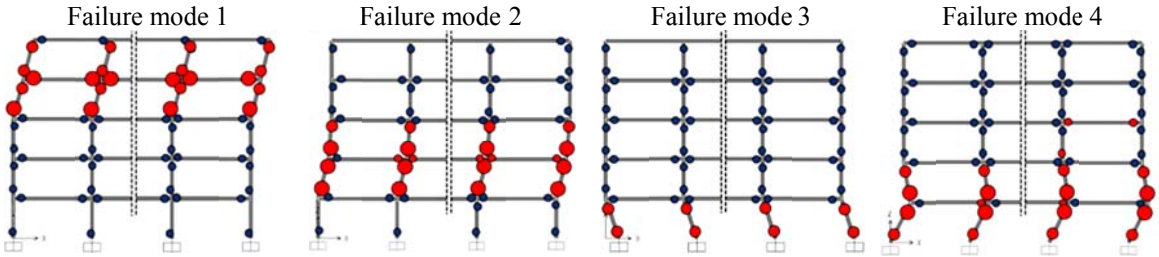

Fig. 14 Collapse modes for RC-MRFs in Class1 and the probability of collapse in each mode

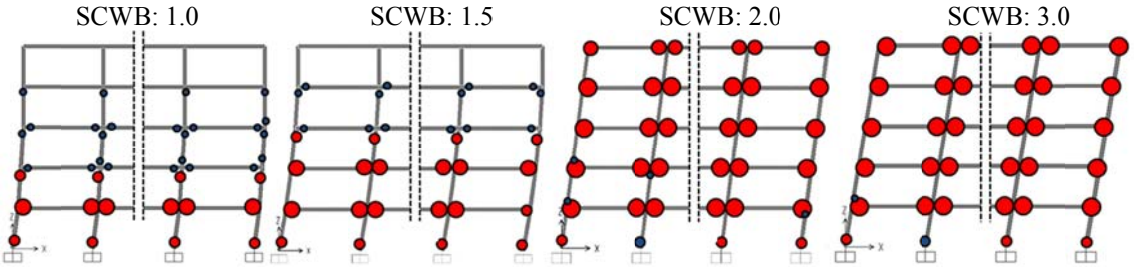

Fig. 15 Predominant collapse mechanisms for RC-MRFs designed with various SCWB ratios

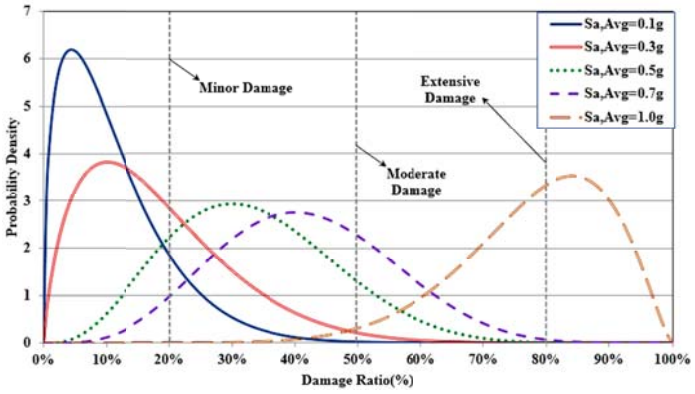

Fig. 16 The probability density distribution of structural damage ratio with different intensities

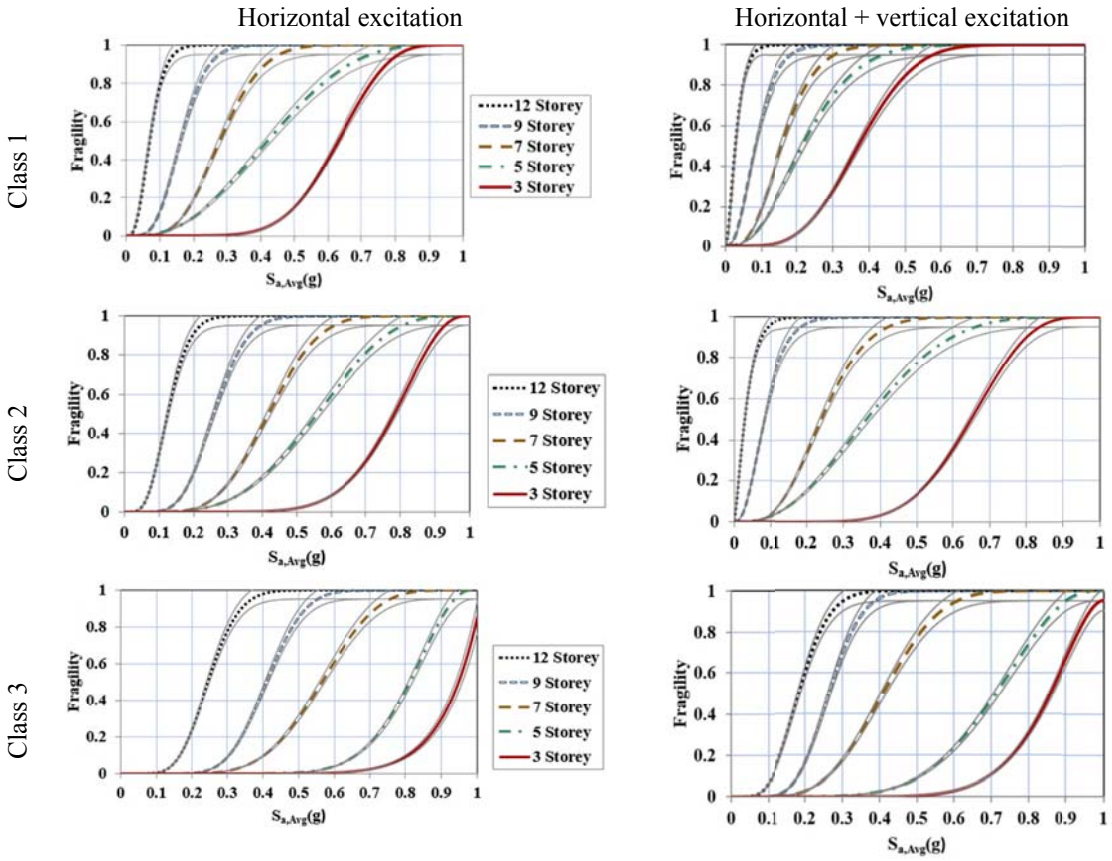

Fig. 17 Fragility curves for various subclasses and No. of storeys under H and H+V excitations

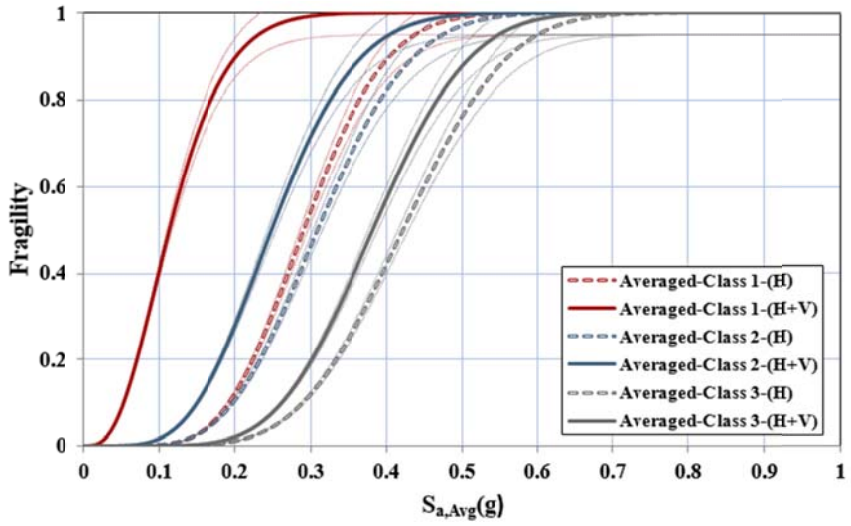

Fig. 18 Averaged fragility curves for various subclasses in moderate damage mode

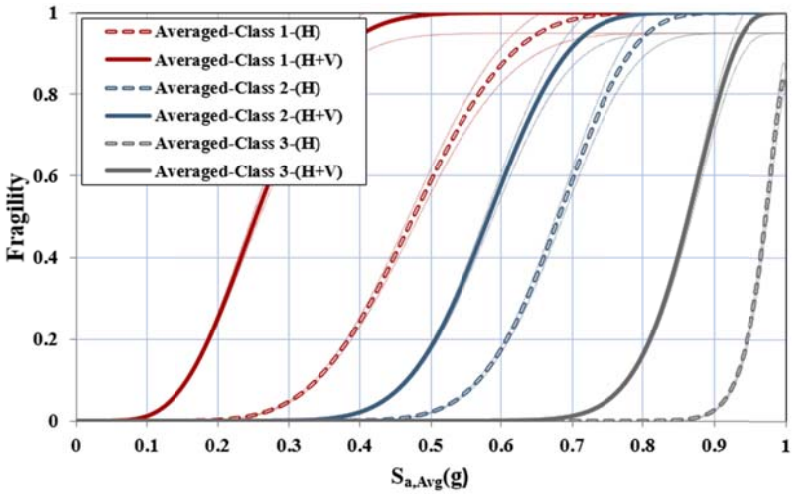

Fig. 19 Averaged fragility curves for various subclasses in collapse mode

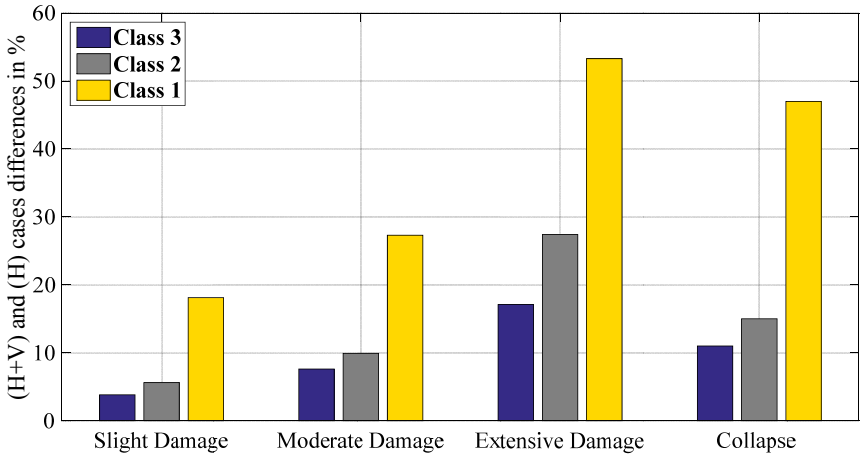

Fig. 20 Fragility estimation increment(%) for combined horizontal-vertical excitations

Table 5 Number of plastic hinges in the beams and columns for horizontal and H+V excitations

States	Horizontal only		H+V, V/H=0.75		H+V, V/H=1.25	
	Beams	*Columns*	*Beams*	*Columns*	*Beams*	*Columns*
Initial hinges in the beams	6	0	9	0	13	0
1st hinge in the 1st storey columns	32	1	41	1	43	4
Development of hinges at all 1st storey columns lower end	39	9	49	22	54	26

arises from uncertain material properties, geometry, quality of construction, and assumptions in structural modeling's of buildings (Kurmann *et al.* 2013).

Fig. 16 shows the probability density distribution of structural damage ratio under various levels of IM and beta fitting distributions for 5 storey typical models. From Fig. 16, it can be seen that choosing beta density distribution function to fit the probability density distribution of

vulnerability matrix can basically express the distribution characteristics of structural damage ratio under determined seismic intensity.

7.10 Fragility estimates considering confidence bounds

Since for practical applications a continuous fragility estimate is preferred, a beta cumulative distribution function is selected to obtain continuous fragility estimates over the entire range of spectral accelerations.

It is desirable to determine the epistemic uncertainty inherent in the fragility estimate, which is reflected in the probability distribution of $F\left(IM;\mu\right)$ relative to the parameter μ. Exact evaluation of this distribution requires nested reliability calculations (Kiureghian 1989). Following Gardoni *et al.* (2002a), approximate confidence bounds are obtained using a first-order reliability analysis. These bounds approximately correspond to 10% and 90% confidence level on the fragility estimates. Fig. 17 show the fragility curves with confidence bounds for all buildings for moderate damage mode (considers as the life safety limit state in the seismic design codes).

As can be seen from Fig. 18, the most difference occurs in the first category buildings (Class 1) and the least is in the 3rd category (Class 3). For a better comparison the collapse fragility curves are as well extracted and illustrated in Fig. 19.

From the extracted fragility curves, it's clear that the effect of vertical component of earthquake cannot be neglected and the most vulnerable buildings are the RC-MRFs in class 1 which usually behave as non-ductile frames. Based on the vulnerability assessment, a two-sample Kolmogorov–Smirnov test has been performed and the fragility discrepancies are calculated.

In the case of multi-component excitations the extracted results have 36.23% (Class 1), 14.46% (Class 2) and 9.87% (Class 3) average differences compared to conventional horizontal excitations. Fig. 20 shows the comparison of the various subclass at the four limit states for all the frame models. The most vulnerable structures are categorized in Class 1 and need immediate retrofitting actions for the future seismic events.

8. Conclusions

In this study, the effect of multi-components seismic excitations including vertical ground motion on the RC-MRFs with 3 subclasses, which represents the majority of residential buildings in Iran, is presented. To generalize the results, 23 RC-MRFs ranging from three to twelve stories, all based on various versions of Iranian Seismic Code (Standard No. 2800) provisions are designed and assessed. Given the fragility curves extracted here, the obvious question is whether these RC buildings meet the intention of current codes and are "safe enough?".

The most important findings are summarized below

1. The ground motion dataset (PEER-NGA) used in this paper implies that higher vertical acceleration tends to create larger V/H ratio. Similar correlation, however, does not exist between the V/H ratio and peak horizontal acceleration.

2. It's shown that selection of an optimal scalar IM will lead to efficiency, sufficiency and scaling robustness. $S_{a,avg}$, is used as an optimal scalar IM to predict inelastic structural response of buildings subjected to recorded ground motions and it's superiority over the conventional IMs is discussed.

3. As the V/H ratio increases, significant increases in axial force variation within the columns are observed. It was also observed that the significant increase of axial force variation due to vertical ground motion leads to an observed reduction of shear capacity as well and increases the potential for shear failure in the vertical members.

4. Another goal of this study was to predict the collapse risk of RC-MRFs located at moderate to high seismic zones of Iran. To realize this goal, a large dataset of ground motions is used and later on, structural models developed and assessed for the collapse failure modes for a large number of RC-MRFs. For the (low and mid)-rise buildings 4 dominant failure modes were observed. Including various SCWB ratios, different collapse modes compared to the previous section are observed.

5. Multi-components seismic excitations including vertical component may alter the collapse mode from flexural to shear failure, and the columns are more susceptible to this type of failure for high amplitude of vertical component of ground motion.

6. The fragility based assessment of the considered buildings suggested that the mid-rise buildings have slightly higher collapse risk than buildings of lower heights.

Taking into account the above observations, RC-MRFs subjected to the concurrent horizontal and vertical seismic excitations could be more vulnerable than those subjected to horizontal ground motions only. Therefore, including vertical ground motion in the analysis is highly recommended for reliable seismic assessment of RC buildings. The topic of acceptable collapse risk and desired safety goals is worthy of substantial further study. Studies such as this can provide better understanding of the collapse safety of current buildings and can inform a decision making process to mitigate risk through the calibration of seismic codes for the design of new buildings.

References

Abrahamson, N.A. and Litehiser, J.J. (1989), "Attenuation of vertical peak acceleration", *B. Seismol. Soc. Am.*, **79**(3), 549-580.

ACI Committee 318 (1989), "ACI 318–89, Building Code Requirements for Structural Concrete", *American Concrete Institute*, Detroit.

ACI Committee 318 (1999), "ACI 318–99, Building Code Requirements for Structural Concrete", *American Concrete Institute*, Detroit.

ACI Committee 318 (2005), "ACI 318–05, Building Code Requirements for Structural Concrete", *American Concrete Institute*, Detroit.

ACI Committee 318 (2011), "ACI 318–11, Building Code Requirements for Structural Concrete", *American Concrete Institute*, Detroit.

Ambraseys, N.N. and Simpson, K.A. (I995), "Prediction of vertical response spectra in Europe", *Research Report ESEE-95/**1***, Imperial College, London.

Applied Technology Council (ATC) (1985), "Earthquake Damage Evaluation Data for California", *Applied Technology Council*, Redwood City, California.

Baker, J.W. (2015), "Efficient analytical fragility function fitting using dynamic structural analysis", *Earthq. Spectra.*, **31**(1), 579-599.

Bentz, E.C. (2000), "Sectional Analysis of Reinforced Concrete Members", Ph.D Thesis, Department of Civil Engineering, University of Toronto.

Bianchini, M., Diotallevi, P.P. and Baker, J.W. (2009), "Prediction of inelastic structural response using an average of spectral accelerations", *Proceedings of the 10th International Conference on Structural Safety and Reliability (ICOSSAR09)*, Arizona, USA.

Borgonovo, E., Zentner, I., Pellegri, A., Tarantola, S. and De Rocquigny, E. (2013), "On the importance of

uncertain factors in seismic fragility assessment", *Reliab. Eng. Syst. Safe.*, **109**, 66-76.
Bozorgnia, Y. and Campbell, K.W. (2004), "The vertical-to-horizontal response spectral ratio and tentative procedures for developing simplified V/H and vertical design spectra", *J. Earthq. Eng*., **8**(2), 175-207.
Broderick, B.M. and Elnashai, A.S. (1995), "Analysis of the failure of Interstate 10 freeway ramp during the Northridge earthquake of 17 January 1994", *Earthq. Eng. Struct. D*., **24**(2), 189-208.
Calvi, G.M., Pinho, R., Magenes, G., Bommer, J.J., Restrepo-Vélez, L.F. and Crowley, H. (2006), "Development of seismic vulnerability assessment methodologies over the past 30 years", *ISET. J. Earthq. Technol.*, **43**(3), 75-104.
Casotto, C., Silva, V., Crowley, H., Nascimbene, R. and Pinho, R. (2014), "Seismic Fragility and Collapse Probability of Italian Precast Reinforced Concrete Industrial Structures", *Proceedings of the 12th International Conference On Computational Structures Technology,* Civil-Comp Press, Stirlingshire, UK.
Cornell, A., Zareian, F., Krawinkler, H. and Miranda, E. (2005), "Prediction of probability of collapse. In H. Krawinkler (Ed.), Van Nuys hotel building testbed report: exercising seismic performance assessment", *Pac. Earthq. Eng. Res*., **11**(4-5), 85-93.
Der Kiureghian, A. (1989), "Measures of structural safety under imperfect states of knowledge", *J. Struct. Eng,-ASCE*., **115**(5), 1119-1140.
Del Gaudio, C., Ricci, P., Verderame, G.M. and Manfredi, G. (2015), "Development and urban-scale application of a simplified method for seismic fragility assessment of RC buildings", *Eng. Struct.*, **91**, 40-57.
Ditlevsen, O. and Madsen, H.O. (1996), "Structural reliability methods", John Wileys & Sons Ltd., Chichester.
Dymiotis, C., Kappos, A.J. and Chryssanthopoulos, M.K. (1999), "Seismic reliability of RC frames with uncertain drift and member capacity", *J. Struct. Eng.-ASCE.*, **125**(9), 1038-1047.
Elnashai, A.S., Papanikolaou, V. and Lee, D. (2004), "Zeus NL-A System for Inelastic Analysis of Structures", *Mid-America Earthquake Center*, University of Illinois at Urbana-Champaign, CD-Release 04-01.
FEMA 273 (1996), "NEHRP Guidelines for the Seismic Rehabilitation of Buildings", *Federal Emergency Management Agency*.
Fujita, K. and Takewaki, I. (2009), "Property of critical excitation for moment-resisting frames subjected to horizontal and vertical simultaneous ground motions", *J. Zhejiang. Univ. Sci. A.*, **10**(11), 1561-1572.
Gardoni, P., Der Kiureghian, A. and Mosalam, K.M. (2002a), "Probabilistic models and fragility estimates for bridge components and systems", PEER Report 2002/13, *Pacific Earthquake Engineering Research Center*, University of California, Berkeley, CA.
Graizer, V. (2006b), "Comparison of Attenuation of Peak Ground Motion and V/H Ratios for California Earthquakes (Abstract)", *Seismol. Res. Lett.*, **77**(2), 324.
Hwang, H. and Huo, J.R. (1997), "Chapter 7.b: Development of Fragility Curves for Concrete Frame and Shear Wall Buildings", Loss Assessment of Memphis Buildings, *Technical Report NCEER 97–0018*, 113-137.
Ibarra, L.F., Medina, R.A. and Krawinkler, H. (2005), "Hysteretic models that incorporate strength and stiffness deterioration", *Earthq. Eng. Struct. D.*, **34**, 1489-1511.
Iranian Standards for Design and Construction of RC Structures, "ABA" & "Part 9", *Building and Housing Research Center*, Tehran, Iran.
Jeon, J.S., Park, J.H. and DesRoches, R. (2015), "Seismic fragility of lightly reinforced concrete frames with masonry infills", *Earthq. Eng. Struct. D*., John Wiley & Sons, Ltd.
Kafali, C. and Grigoriu, M. (2004), "Seismic fragility analysis", *Proceedings of the 9th ASCE Specialty Conference on Probabilistic Mechanics and Structural Reliability.*
Kennedy, R.P. and Ravindra, M.K. (1984), "Seismic fragilities for nuclear power plant risk studies", *Nucl. Eng. Des.*, **79**(1), 47-68.
Kim, S.H. and Shinozuka, M. (2004), "Development of fragility curves of bridges retrofitted by column jacketing", *Probabilist. Eng. Mech.*, **19**(1-2), 105-112.
Kurmann, D., Proske, D. and Cervenka, J. (2013), "Seismic fragility of a reinforced concrete

structure", *Kerntechnik.*, **78**(2), 120-126.
Lee, T.H. and Mosalam, K.M. (2004), "Probabilistic fiber element modeling of reinforced concrete structures", *Comput. Struct.*, **82**(27), 2285-2299.
Lee, D.H. and Elnashai, A.S. (2001), "Seismic Analysis of RC bridge columns with flexure shear interaction", *J. Struct. Eng.-ASCE.*, **127**(5), 546-553.
Lee, Y.J. and Moon, D.S. (2014) "A new methodology of the development of seismic fragility curves" *Smart. Struct. Syst.*, **14**(5), 847-867.
Luco, N. and Cornell, C.A. (2007), "Structure-specific scalar intensity measures for near-source and ordinary earthquake ground motions", *Earthq. Spectra.*, **23**(2), 357-392.
Mander, J.B., Priestley, M.J.N. and Park, R., (1988), "Theoretical stress-strain model for confined concrete", *J. Struct. Eng.-ASCE.*, **114**(8), 1804-1826.
Mazzoni, S., McKenna, F., Scott, M.H., Fenves, G.L. and Jeremic, B. (2007), "Open sees command language manual", The Regents of the University of California.
Newmark, N.M., Blume, J.A. and Kapur, K.K. (1973), "Seismic design spectra for nuclear power plants", *J. Power. D.*, **99**(2), 287-303.
Porter, K., Kennedy, R. and Bachman, R. (2007), "Creating fragility functions for performance-based earthquake engineering", *Earthq. Spectra.*, **23**(2), 471-489.
Ramamoorthy, S.K., Gardoni, P. and Bracci, J.M. (2006a), "Probabilistic demand models and fragility curves for reinforced concrete frames", *J. Struct. Eng.-ASCE.*, **132**(10), 1563-1572.
Shafei, B., Zareian, F. and Lignos, D.G. (2011), "A simplified method for collapse capacity assessment of moment-resisting frame and shear wall structural systems", *Eng. Struct.*, **33**(4), 1107-1116.
Shome, N., Cornell, C.A., Bazzurro, P. and Carballo, J.E. (1998), "Earthquakes, records, and nonlinear responses", *Earthq. Spectra.*, **14**(3), 469-500.
Schotanus, M.I.J., Franchin, P., Lupoi, A. and Pinto, P.E. (2004), "Seismic fragility analysis of 3D structures", *Struct. Saf.*, **26**(4), 421-441.
SEAOC (1995), "Performance Based Seismic Engineering of Buildings", *Vision 2000 Committee*, Structural Engineers Association of California, Sacramento, California.
Sinozuka, M., Feng, M.Q., Kim, H.K. and Kim, S.H. (2000), "Nonlinear static procedure for fragility curve development", *J. Eng. Mech.-ASCE.*, **126**(12), 1287-1295.
Song, J. and Ellingwood, B.R. (1999), "Seismic reliability of special moment steel frames with welded connections: II", *J. Struct. Eng.-ASCE.*, **125**(4), 372-384.
Standard No. 2800 V.1 (1988), "Iranian Code of Practice for Seismic Resistant Design of Buildings", *Building and Housing Research Center*, Tehran, Iran.
Standard No. 2800 V.2 (1999), "Iranian Code of Practice for Seismic Resistant Design of Buildings", *Building and Housing Research Center*, Tehran, Iran.
Standard No. 2800 V.3 (2005), "Iranian Code of Practice for Seismic Resistant Design of Buildings", *Building and Housing Research Center*, Tehran, Iran.
Sudret, B., Mai, C. and Konakli, K. (2014), "Computing seismic fragility curves using non-parametric representations", *Struct. Saf.*, arXiv:1403.5481v2 [stat.AP] 4.
Vamvatsikos, D. and Cornell, C.A. (2002), "Incremental dynamic analysis", *Earthq. Eng. Struct. D.*, **31**(3), 491-514.
Vecchio, F.J. and Collins, M.P. (1986), "The Modified Compression Field Theory for Reinforced Concrete Elements Subjected to Shear", *ACI. Struct. J.*, **83**(2), 219-231.
Villaverde, R. (2007), "Methods to assess the seismic collapse capacity of building structures: State of the art", *J. Struct. Eng.-ASCE.*, **133**(1), 57-66.

CC

Nomenclature

C :	Probabilistic structural capacity
D :	Probabilistic structural demand
μ :	Uncertainties in structural demand
M_w :	Moment magnitude of a seismic event
V/H :	Peak vertical to horizontal ground acceleration
Θ_p :	Plastic rotation capacity
Θ_{pc} :	Post-Capping plastic rotation capacity
Θ_c :	Capping rotation capacity
Θ_y :	Effective yield rotation
Θ_r :	Corresponding rotation to residual strength
Θ_u :	Ultimate rotation capacity
K_e :	Effective elastic stiffness
M_r :	Residual strength
M_y :	Effective yield strength
M_c :	Capping strength
T_1 & T_n :	Lower and upper period bounds to calculate the geometric spectral acceleration
$T^{(1)}$:	Fundamental period of the structure
k_1 & k_u :	constants specifying lower and upper bounds
T_{low} & T_{upp} :	Lower and the upper periods of the elastic spectrum
Δ_i :	Absolute displacement of the *i*th storey
ε_{cc} :	Concrete strain corresponding to maximum confined concrete stress
ε_{co} :	Concrete strain corresponding to maximum unconfined concrete stress
f'_{cc} :	Maximum confined concrete stress
f'_{co} :	Maximum unconfined concrete stress
ε_{cu} :	Maximum confined concrete strain
α :	Confinement effectiveness coefficient for the model proposed by (Mander et al. 1988)
ω_w :	Mechanical volumetric ratio of confining hoop
w_i :	*i*th clear transverse spacing between adjacent longitudinal bars
A_{cc} :	The area of the confined concrete
α_n & α_s :	parameters defined to simplify the α presentation
S :	Stirrup spacing
d_c :	Concrete core dimension to center line of perimeter hoop